Sandstorm erosion simulation on solar mirrors and comparison with field data

Florian Wiesinger, Florian Sutter, Fabian Wolfertstetter, Natalie Hanrieder, Johannes Wette, Aránzazu Fernández-García, and Robert Pitz-Paal

Citation: AIP Conference Proceedings **1850**, 130014 (2017);

View online: https://doi.org/10.1063/1.4984508

View Table of Contents: http://aip.scitation.org/toc/apc/1850/1

Published by the American Institute of Physics

Sandstorm Erosion Simulation on Solar Mirrors and Comparison with Field Data

Florian Wiesinger[1, a)], Florian Sutter[1], Fabian Wolfertstetter[1], Natalie Hanrieder[1], Johannes Wette[1], Aránzazu Fernández-García[2] and Robert Pitz-Paal[3]

[1]*DLR German Aerospace Center, Address: Institute of Solar Research, Plataforma Solar de Almeria, Ctra. Senés, km.4, P.O. Box 39, 04200 Tabernas, Almería, Spain.*
[2] *CIEMAT-Plataforma Solar de Almería, Ctra. Senés, km 4, P.O. Box 22, 04200 Tabernas, Almería, Spain*
[3] *DLR German Aerospace Center, Institute of Solar Research, Linder Höhe, 51147 Cologne, Germany*

[a)]Corresponding author: florian.wiesinger@dlr.de

Abstract. Solar reflectors for concentrating solar power applications can be subject to performance losses due to their permanent exposure to the environment. In this work the risk of erosion due to sandstorms is evaluated. Aluminum and glass reflector samples were exposed in Missour and Zagora (Morocco) and measurements of the wind velocity and the particle concentration were carried out. Both measured quantities were connected to the single particle momentum distribution SPMD. This novel parameter is shown to be adequate to describe the erosion characteristics of outdoor sites and laboratory setups. Its deduction will be explained and it will be applied to both outdoor sites and two accelerated erosion simulation setups, a sand trickling device -named soil pipe- and a closed loop wind channel with particle injection. Furthermore different erosion failure modes are described and explained by the use of the SPMD.

INTRODUCTION

To guarantee the long-term efficient operation of Concentrating Solar Power (CSP) plants, the durability of the reflectors is of major importance. Various meteorological factors of the potential plant site need to be taken into account and accelerated aging tests are carefully chosen to correspond to the natural effects that might take place on the respective components. Usually the assessment of optical materials for particular plant sites is carried out by standardized aging tests like the salt spray test according to ISO 9227 [1] for maritime environment, the ISO 11507 [2] standard for long-term UV-radiation and cyclic condensation or the IEC 61215 [3] standard for the simulation of thermal cycles. However there is still a lack of experience regarding the destructive effects of sand- and duststorms on reflector materials. No accelerated aging guideline is formulated yet to account for the performance loss of solar mirrors due to particle erosion to a realistic extent. The majority of CSP plants are located or planned in desert regions. Therefore an increasing number of plant operators become aware of the threat of erosion due to wind carried particles and ask for testing procedures to perform optimized risk analysis for their energy output and cost calculations, since the service life times of reflectors are aimed to be at 10-30 years [4].

Wette et al [5] found that reflectance losses of aluminum reflectors provoked by outdoor aging vary significantly for different outdoor sites. Even though in a less pronounced way, this is assumed to be true for glass reflectors as well. In the current study we investigate the meteorological and geological particle characteristics that are presumed to influence the degradation rate of the samples. The sites Zagora and Missour (both in Morocco) have been selected because of the different reflectance losses that have been observed there. In addition Morocco is now heavily investing in the CSP sector, following the ambitious plan to have installed 2000 MW of solar capacity by 2020 [6].
The main erosion determining factors have already been identified in several previous studies [7-16]. In the following they are listed together with a short explanation and scientific works that have been dedicated to the investigation of the respective parameters:

SolarPACES 2016
AIP Conf. Proc. 1850, 130014-1–130014-10; doi: 10.1063/1.4984508
Published by AIP Publishing. 978-0-7354-1522-5/$30.00

- Velocity of the particles. The wind velocity is taken as a standard measure for that quantity.
- Concentration of particles or mass flux to determine the amount of impacting particles.
- Shape of the impacting particles.
- Hardness of the impacting particles. Since it's not feasible to determine the global hardness of a powder with different components, the mineralogical composition and the hardness of each single component is often taken as a measure.
- The angle of attack or the impact angle α under which the particles are impacting upon the surface of the reflector (α = 90° stands for perpendicular impact).

In the first part of the paper the analysis of the outdoor data is performed. Afterwards the results from the accelerated laboratory erosion setups will be discussed and compared to the data from Missour and Zagora.

METHODOLOGY

In this chapter, the sensors that were deployed in the field are presented and the setups that were used in the laboratory for artificial aging are described. To compare the natural and artificial erosion effects, the monochromatic specular reflectance, ρ_λ (660 nm, 15°, 12.5 mrad) and the respective loss from its initial value $\rho_{\lambda,loss}$, was measured with the Devices and Services (Dallas, USA) (D&S) R15 reflectometer and an optical inspection has been performed with an Axio CSM 700 microscope by Zeiss (Oberkochen, Germany).

Meteorological Data from Outdoor Sites

The meteorological and geological data presented in this work has been acquired at two stations (see Fig. 1a) close to Zagora (30°19′50′′ N, 5°50′17′′ W) and Missour (32°53′46′′ N, 4°06′37′′ W), both in Morocco. The two stations belong to the enerMENA meteorological network [17, 18]. The reflector samples are mounted at a tilt angle of 45° facing south in a height between 1 and 1.5 m above ground level. The direct normal irradiance (DNI) is measured with a rotating shadow band irradiometer (type: RSP-4G manufactured by Reichert GmbH) in Zagora. In Missour, a solar tracker with mounted CHP1 pyrheliometer by Kipp & Zonen (Delft, Netherlands) is installed. Temperature and relative humidity are measured by a Campbell Scientific CS100 (Logan, Utah, USA) and the wind velocity and direction at 10 m height is measured with a #40C and a #200P from NRG (Hinesburg, Vermont, USA), respectively. An EDM164 manufactured by GRIMM Aerosol Technik GmbH&Co.KG (Ainring/Germany) (Fig. 1c) has been mounted at a sampling height of around 1 m. This instrument counts airborne particles with diameters ranging from 0.25 to 1200 µm by light scattering optics. It differentiates between 31 size channels where the largest one counts all the particles with a diameter larger than 32 µm. The evaluation will only be performed up to particle diameters of 31 µm, in order not to lose accuracy because of the poor sampling efficiency of this instrument at larger particle sizes that other scholars pointed out already [19].

The exposed reflector materials are first surface aluminum reflectors and second surface silvered-glass reflectors. They have been investigated after 24 month of outdoor exposure.

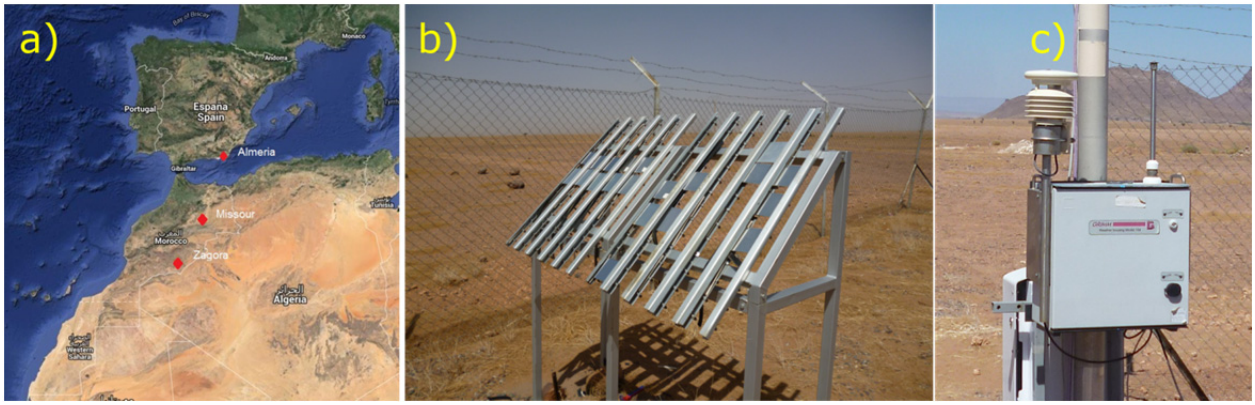

FIGURE 1. (a) Location of outdoor exposure sites in Morocco and Spain at the Plataforma Solar de Almería (PSA); (b) Outdoor exposure rack with reflectors in Zagora; (c) EDM164 particle counter from Grimm that was used on both sites to measure the particle concentration (location in this picture: Zagora).

Artificial Laboratory Aging Setups

One laboratory setup, the soil pipe (see Fig. 2a), is applied to simulate erosion effects artificially. The device has been developed according to DIN 52348 [20] and has been examined in more details in a previous work [16]. It consists of a vertical pipe with included meshes to guarantee a homogeneous sand distribution and a rotating sample holder. The impact angle α is adjustable from 0° to 90°. The used erosion material is synthetic quartz sand with a particle distribution between 300 and 625 µm. The impact velocity of the sand particles in this setup has been determined to be between 2.5 and 4.0 m s^{-1}. Because this parameter could not be changed within the setup and it was not possible to use an erosion material with a size distribution in the smaller diameter range (for explanation it may be referred to [16]) the sandstorm chamber (SSC, see Fig 2b)) was used for further erosion testing. It is a closed channel where the wind velocity can be adjusted between 5.0 and 30.0 m s^{-1} by a centrifugal fan blower. The erosion material is synthetic quartz sand with a particle distribution at a maximum of 180 µm after ISO 12103-1 A4 [21]. The dust injection is facilitated by a compressed air mechanism and the average concentration present in the chamber is determined via a gravimetrical bypass technique.

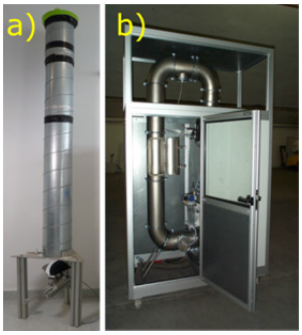

FIGURE 2. Artificial erosion setups in the laboratory. (a) Soil pipe, like proposed in DIN 52348 [20] and (b) closed loop SSC.

RESULTS AND DISCUSSION

Outdoor Measurements

The evaluation of the average specular reflectance losses of various aluminum mirrors exposed for 24 months (from June 2013 to June 2015) delivered values of 36.9% and 5.1% for Zagora and Missour, respectively. For exposed glass mirrors, the average specular reflectance losses have been measured to be 10.8% and 0.8% for Zagora and Missour after an exposure of 24 months. Microscope pictures of the samples that depict the observed defects can be seen in Fig.3 where they are compared to the effects that could be generated with the artificial aging setups.

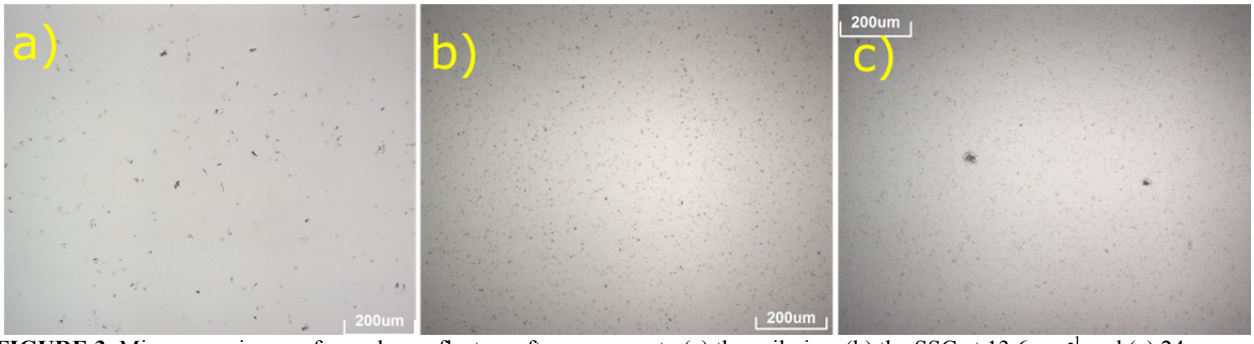

FIGURE 3. Microscope images from glass reflectors after exposure to (a) the soil pipe, (b) the SSC at 13.6 m s^{-1} and (c) 24 months in Zagora.

Even though aluminum mirrors also suffer from reflectance losses due to corrosion or delamination of coatings [22], the elevated erosion on the Zagora site becomes clear from the reflectance losses of glass and the pictures

shown in Fig.3. In the following paragraph an investigation on the parameters that were listed in the introduction as erosion- determining is presented.

TABLE 1. Temporal frequency of the wind speed in Zagora and Missour for the period of June 2014 to July 2016. Directional frequency is displayed in the respective wind rose diagram.

wind speed range [m s^{-1}]	frequency in Zagora [%]	frequency in Missour [%]
v < 6	50.19	54.69
6 < v < 10	41.72	37.92
10 < v < 15	7.32	6.46
15 < v < 20	0.75	0.89
20 < v	0.01	0.05

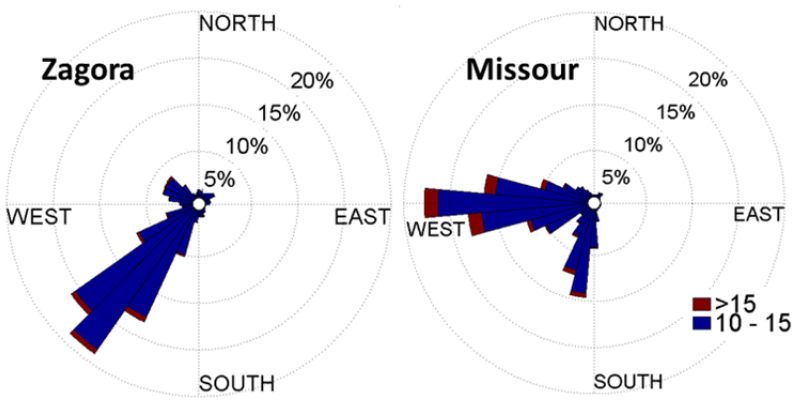

An evaluation for the relative frequency of the various wind speed ranges can be seen in Table 1. Low wind speeds are present in more than 50% of the time at both sites. The occurrence of velocities higher than 10 m s^{-1} is also in the same frequency range. However it is worthwhile to note, that very strong wind events with wind speeds exceeding 20 m s^{-1} are more than 5-times more common in Missour as in Zagora. From the wind rose diagrams the most usual wind directions at velocities over 10 m s^{-1} are illustrated. In Zagora the most significant part of severe wind events is blowing from southwest directions. In Missour, for strong wind speed portions, mostly west direction has been measured and only a small contribution is coming from the south.

Besides the wind velocities also the dust concentration from EDM164 measurements has been evaluated. In Fig. 4 the calculated total suspended particle (TSP) concentration is shown. It has been derived from the particle number distribution measurement according to

$$TSP(t) = \sum_i N_i(t) \cdot V_i \cdot \rho / V_a \qquad 1)$$

where N_i corresponds to the number of particles in the respective size channel *i*, V_a is the air volume, V_i is the volume of the particles and ρ is the density which was assumed to be 2.5 g cm^{-3}. The particles were assumed to be spheres with diameters corresponding to the size channels *i*. This is a prevalent assumption [23], although dust particles are of non-spherical shape.

Figure 4a) illustrates the temporal evolution of the TSP concentration from the beginning of April to the end of June 2016. Usually the TSP values do not exceed 1000 µg m^{-3} in Zagora and Missour but during severe wind events maximum values of 404102 and 38283 µg m^{-3} could be detected, respectively. In order to have a more detailed view on the TSP range distribution, Fig 4b) depicts the frequency of occurrence for different TSP concentration bins. While for Missour the TSP concentration is higher than 100 µg m^{-3} for around 10% of the period, this is the case for about 35% in Zagora. The frequency of extreme dust concentration events is significantly higher in Zagora. From these data it can be concluded, that on average more particles are dissolved in the air in Zagora what increases the probability of impacts on the exposed reflector materials.

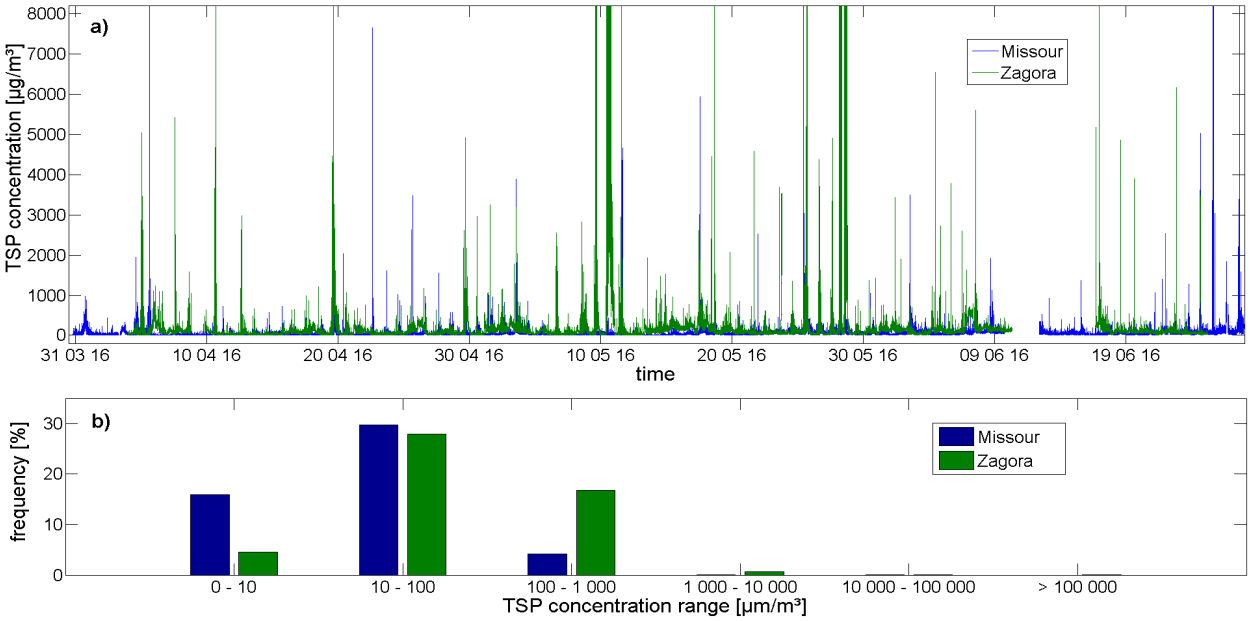

FIGURE 4. TSP values calculated from particle number distribution measured with Grimm EDM 164; (a) temporal presentation of the TSP concentration of the two sites and (b) frequency of different size ranges in the investigated timeframe.

In Fig. 5 the average particle number size distributions (PSD) for diameters between 0.25 and 31 µm are shown for different TSP ranges, e.g. the blue line shows the average PSD measured at a TSP concentrations between 0 and 10 µg m^{-3}. It can be seen that on average, the number of particles in each channel increases with increasing TSP. The PSD can be converted to relative particle volume distribution PVD_{rel} by multiplying each particle size channel with its respective volume and normalizing it to the total measured volume of each timestamp. PVD_{rel} was evaluated for each TSP bin and is shown in Fig. 5b). For low TSP concentrations the volumetric proportion of particles with diameters larger than 10 µm is less pronounced than for larger particles. The latter constitute the major portion of the total measured particle volume per unit air volume. It is important to note, that for high TSP events not only the number of total suspended particles is increasing but also the percentage of bigger particles is augmented disproportionately strong.

The parameters of PSD and wind velocity can be connected to the single particle momentum SPM_i, calculated according to

$$SPM_i(t) = m_i(t)\vec{v}(t) = m_i(t)v(t)\cdot\cos 45^\circ\cdot\cos\beta(t) \qquad 2)$$

with m_i being the mass of a particle in channel i and $\vec{v}$ the wind vector at the time of measurement, t. As a whole, the SPM_i form the single particle momentum distribution function SPMD, i.e. the distribution of momenta for each point in time. The two cosines take into account the impact angle between the reflector sample and the windblown particles. It is assumed that the wind has a horizontal component only, that the particles are traveling with the same velocity and direction as the air and that the wind direction relative to the normal component of the surface normal vector of the mirror is β.

Furthermore it should be stated, that due to the measurement point of v (10 m above ground) the actual SPMD should be slightly lower. In undisturbed wind fields the wind velocity height profile can be approximated by the model of Karman [24]. The model describes a logarithmic increase of wind velocity with height above ground. If a surface roughness length z_0 of 0.005 is assumed, this would result in a 20% lower absolute wind velocity at reflector height in comparison to the wind velocity measurement height. The momentum has been calculated for all detected particles in Zagora and Missour and has been segmented in different momentum channels. Taking into account that at higher wind speeds, more particles are blown towards the surface, the number of particles of a point in time for each momentum channel is scaled linearly with the wind velocity. The graph in Fig.6 displays the relative number of impacts in a certain momentum range normalized to the total number of measured impacts. While in Missour most

momenta lay in the region of 10^{-13}, the *SPMD* peaks in Zagora at around 10^{-12} g m s^{-1}. Furthermore it needs to be stated, that the chance of impact with high momentum (between 10^{-7} and 10^{-6} g m s^{-1}) is elevated by a factor of around 10 in Zagora when compared to Missour. To cause permanent defects in glass reflectors, impacts with high momentum are more effective than impacts by small particles with low velocity [7]. Hence this difference in *SPMD* could explain the variations in erosion severeness of the two investigated sites. It needs to be stated that the evaluation could only be executed for particle diameters smaller than 31 µm. Larger particles certainly have been present during some events, could not be detected due to the limited size range of the EDM164 and the low collection efficiency in size ranges of diameters larger than 31µm [19]. However particles with diameter significantly larger than 31 µm could be proven to be present by the use of adhesive tapes at various heights above ground, where windblown particles have been captured and examined in the laboratory via optical microscopy. Other scholars like Hutchings [25] and Shipway et al. [26] suggested that there is a threshold value for particle properties to cause erosion. This could especially be true for the particle diameter, since it scales to the impact energy to the power of three and the work by Routbourt et al.[27] suggests that the threshold size range is likely to be found in the order of magnitude where the measurements took place. Therefore it is reasonable to assume that the contribution of the smallest detected particles by the EDM164 to the erosion effects is very little. Still it has been decided to present them in the evaluation in order to get a general idea about the PSD of aeolian particles and because it was not possible to exactly determine the threshold value.

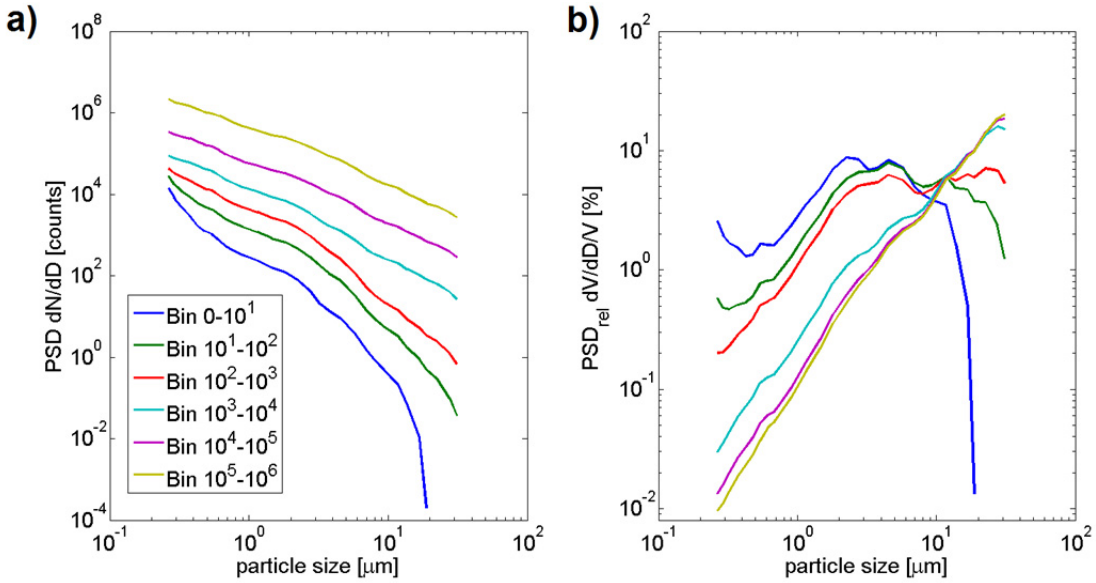

FIGURE 5. Average particle size distributions over different *TSP* concentration bins measured in Zagora. Bin 1 stands for events with TSP concentration between 0 and 10 and bin 6 for the TSP concentration larger than 100000 µg m^{-3}, respectively; (a) depicts the number of counts of the Grimm device in each of its size channels and (b) the resulting normalized volume distribution.

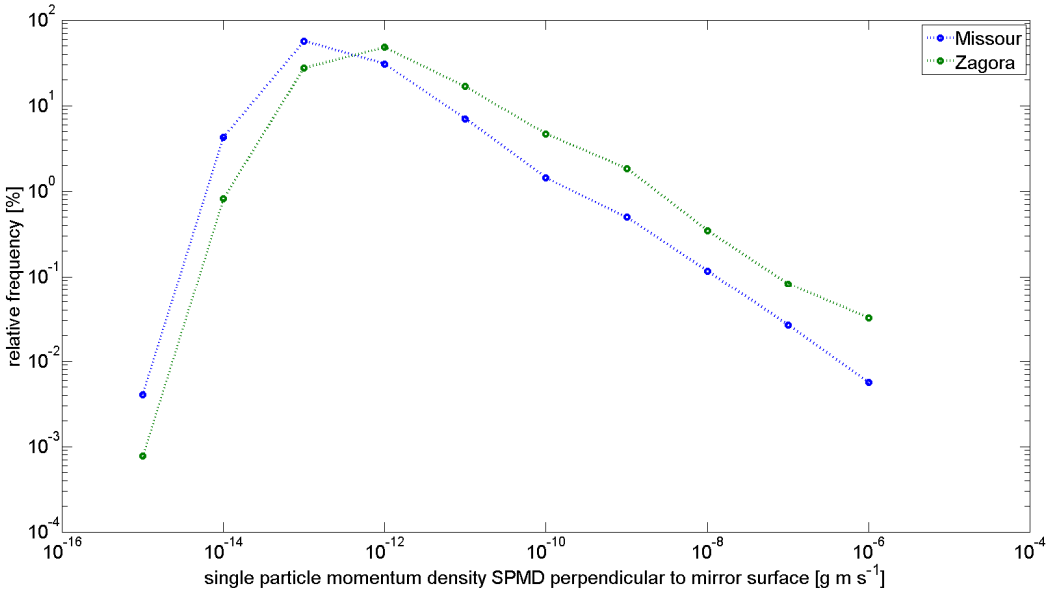

FIGURE 6. Relative frequency of *SPMD* perpendicular to mirror surface. The total number of impacts evaluated for this relative frequency representation was $3.2 \cdot 10^{12}$ and $10.0 \cdot 10^{12}$ for Missour and Zagora respectively.

Artificial Aging

Microscope pictures of glass samples that have been artificially eroded are shown in Fig 3 and are compared to a sample that was exposed for 24 months in Zagora. The reflector sample tested in the soil pipe exhibits several defects in the size range of 10 µm in diameter and larger (Fig. 3a)). Defects of this size can also be found on the sample exposed in Zagora (Fig. 3c) but the majority of the defects caused by natural erosion are by one order of magnitude smaller. The artificially erosion treatment in the SSC does only provoke defects in this smaller size range only (see Fig. 3b).

The soil pipe is a simple setup and erodes tested mirror samples in a very uniform way. The specular reflectance loss correlates with the used sand mass linearly. It has been possible to ascribe characteristic erosion resistances to different sample types (for details see [16]). As it is displayed in Fig. 7a) the setup could be used to determine the dependence of the specular reflectance loss on the impact angle α. It is maximal for perpendicular impacts and decreases with α becoming smaller than 90°.

The SSC was used to determine the influence of v on the severeness of artificial erosion treatment. In Fig. 7b) $\rho_{\lambda,loss}$ was plotted for two different v. Also in this setup the specular reflectance loss scales linearly with the total used sand mass. Increasing v from 7.6 to 13.6 m s^{-1} leads to an amplification of erosion severeness of a factor of five.

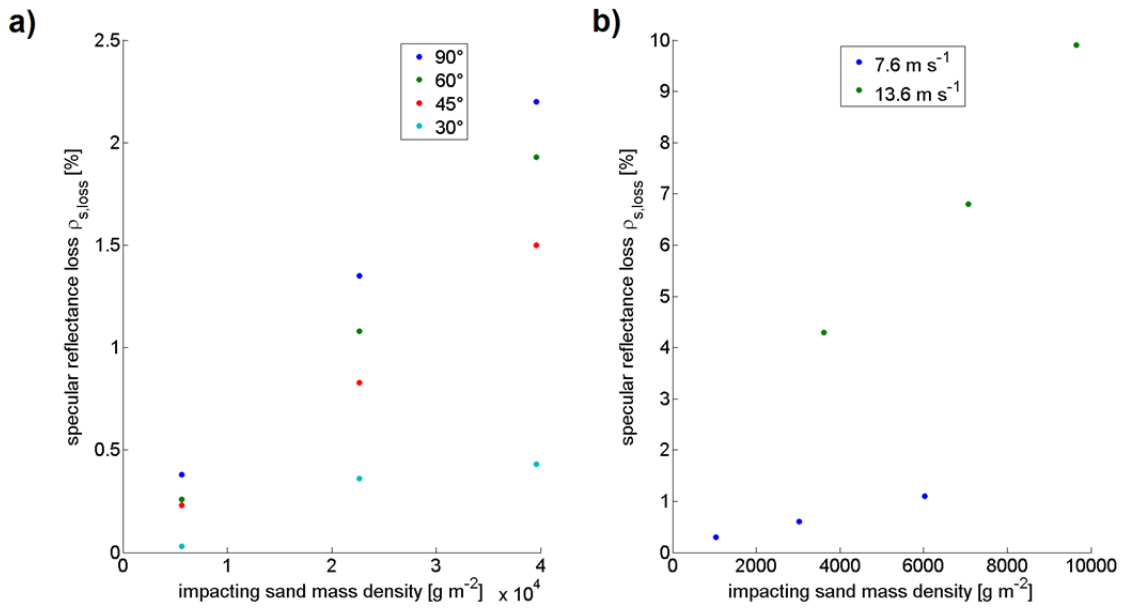

FIGURE 7. Artificially provoked specular reflectance losses of glass mirrors for increasing impacting sand mass in (a) the soil pipe setup for different α and (b) the sandstorm chamber for different *v*.

The investigated setups lead to erosion effects on the reflector samples that are also present on naturally eroded samples. Furthermore, it is possible to reach similar $\rho_{\lambda,loss}$ as observed in the field by the application of both setups and the simple adjustment of the used sand mass. A $\rho_{\lambda,loss}$ of 10.8%, as measured in Zagora after 24 months, corresponds to the application of a total sand mass density of $2.0 \cdot 10^5$ g m^{-2} in the soil pipe with α equal to 90° or $1.2 \cdot 10^4$ g m^{-2} in the SSC at *v* equal to 13.6 m s^{-1}. The reason for this significant difference of used sand mass to cause the same loss of specular reflectance is the crucial difference of the physical parameters of both erosion materials. The resulting SPMD is illustrated in Fig. 8 for the treatment in the soil pipe and the SSC. The parameters on which the calculations are based are given in the caption. Furthermore the cumulated SPMD for 24 months in Zagora and Missour is presented in Fig.8 for comparison as well. It can be seen that neither the soil pipe nor the SSC can reproduce impacts exhibiting momenta smaller than 10^{-10} g m s^{-1}. Though most of the impacting momenta outdoor are measured in this range, it is not regarded as problematic since those impacts are not considered to cause erosion defects. The momenta present in the soil pipe are three to four magnitudes larger than those observed in the field and fewer particles impacted on the sample. This can explain the different failure mode observed already by the microscope images. The SPMD for the SSC does overlap in a certain momentum range and the total amount of impacts in this range is also comparable to the total frequency determined for two year exposure time at the outdoor sites. In particular the SPMD for the SSC would coincide well with the extrapolation of the SPMD of Zagora to higher momenta. Due to the restrictions of the size sensitivity of the dust measuring device they could not be determined reasonably. The good agreement of $\rho_{\lambda,loss}$ and optical inspection via microscope between the SSC results and the samples from outdoor sites supports the theory that mainly high momentum impacts are responsible for permanent erosion damage.

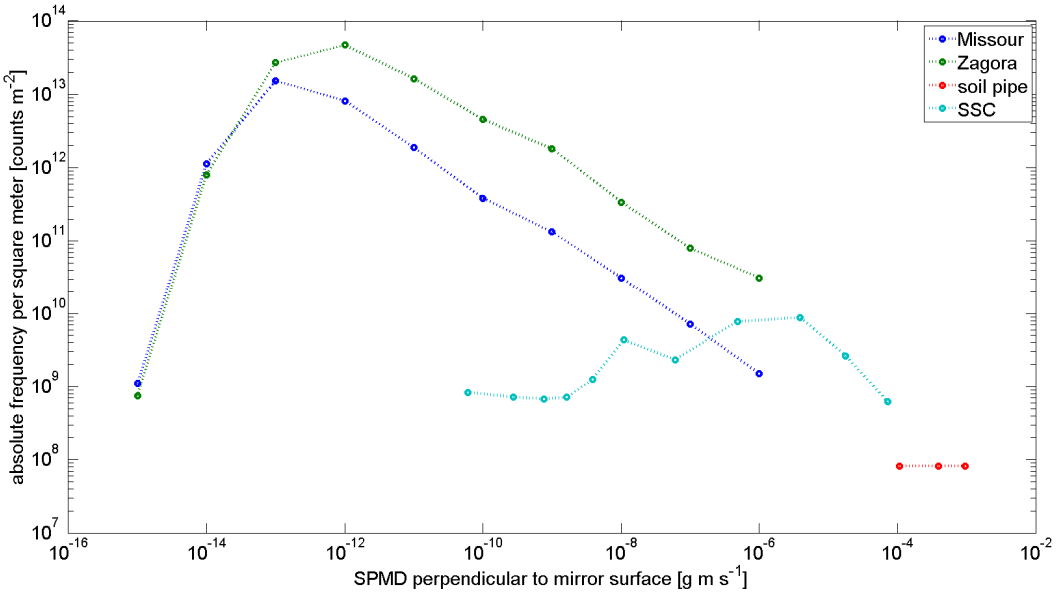

FIGURE 8. Absolute frequency of SPMD over 24 months for Missour and Zagora has been obtained by extrapolating the data from the 2.5 month of Grimm measurements to the full 24 month period. The SPMD for the ISO 12103-A4 dust in the SSC was calculated a velocity of 13.6 m $^{-1}$ and after a total impact mass of $9.7 \cdot 10^{3}$ g m^{-2}. The SPMD for the quartz particles in the soil pipe was calculated with a velocity of 3 m s^{-1} and after a total impact mass of $4 \cdot 10^{4}$ g m^{-2}. Note that the total number of impacts (counts) is different for each curve. The data for Missour and Zagora represent the calculated number of impacts during the complete exposure period.

CONCLUSION AND OUTLOOK

Within this paper two outdoor sites in Morocco have been analyzed in matters of their erosion characteristics. Wind velocities and direction has been evaluated as well as the aeolian particle size distribution. From both physical quantities the single particle momentum density SPMD has been derived. This variable is considered as a promising parameter to compare various sites and also laboratory setups regarding erosion behavior. However it was not possible to take into account particles bigger than 31 µm in the evaluation for the outdoor sites. Since the momentum scales with the cube of the particle diameter it would be highly desirable to detect them as well during the next measurement campaign. This will be accomplished by the application of a gravimetrical dust sampler deployed at Zagora. Regarding the artificial setups an open loop wind channel has already been constructed to facilitate accelerated erosion experiments with different test dusts to determine the influence of particle hardness and particle shape on the erosion effects.

ACKNOWLEDGMENTS

The research leading to these results has received funding from the European Union Seventh Framework Programme (FP7/2007-2013) under Grant Agreement no.609837 (Scientific and Techno-logical Alliance for Guaranteeing the European Excellence in Concentrating Solar Thermal Energy, STAGE-STE). The authors want to thank Tomás Jesús Reche Navarro (DLR) for his support.

REFERENCES

1. ISO 9227, Corrosion Tests in Artificial Atmospheres - Salt spray test, International Organization for Standardization, (2006).
2. ISO 11507, Paints and Varnishes - Exposure of Coatings to Artifical Weathering - Exposure to Fluorescent UV Lamps and Water, International Organization for Standardization, (2013).

3. ISO 61215, Crystalline Silicon Terrestrial Photovoltaic (PV) Modules - Design Qualification and Type Approval, International Electrotechnical Commission, (2005).
4. A. García-Segura, A. Fernández-García, M.J. Ariza, F. Sutter, L. Valenzuela, Durability studies of solar reflectors: A review, *Renewable and Sustainable Energy Reviews*, 62, 453-467 (2016).
5. J. Wette, F. Sutter, A. Fernández-García, Correlating outdoor exposure with accelerated aging tests for aluminum solar reflectors, AIP Conference Proceedings, 1734 (2016) 090003.
6. https://www.technologyreview.com/s/600751/moroccos-massive-desert-solar-project-starts-up/
7. E.G. Collier, Development and use of a duststorm simulation chamber to evaluate solar concentrator degradation as characterized by loss in reflectivity, Master Thesis, Texas Tech University, 1980.
8. A.M. Cooper, Development of an improved, accelerated test for the effect of blowing dust on the service-life of solar collectors, Master Thesis, Texas Tech University, 1985.
9. C. Sansom, P. Comley, P. King, H. Almond, C. Atkinson, E. Endaya, Predicting the effects of sand erosion on collector surfaces in CSP plants, SolarPACES Bejing,2014.
10. C. Völker, D. Philipp, M. Masche, T. Kaltenbach, Development of a test method for the investigation of the abrasive effect of sand particles on components of solar energy systems, Proceedings of the European PV Solar Energy Conference 2014, Amsterdam, 2014.
11. M. Karim, S. Naamane, C. Delord, A. Bennouna, Laboratory simulation of the surface erosion of solar glass mirrors, *Solar Energy*, 118, 520-532 (2015).
12. S. Bouzid, Z. Azari, Impact depth on glass surface caused by sand particles, *Applied Mechanics and Materials*, 146, 197-212 (2012).
13. R. Zakhidov, A. Ismanzhanov, Investigation of abrasive action of atmospheric particles on the reflectance of mirrors, *Appl. Solar Energy*, 16(6), 43-47 (1980)..
14. N. Bouaouadja, S. Bouzid, M. Hamidouche, C. Bousbaa, M. Madjoubi, Effects of sandblasting on the efficiencies of solar panels, *Applied energy*, 65, 99-105 (2000).
15. R. Bethea, E. Collier, J. Reichert, Dust storm simulation for accelerated life testing of solar collector mirrors, *Journal of solar energy engineering*, 105, 329-335 (1983).
16. F. Wiesinger, F. Sutter, A. Fernández-García, J. Reinhold, R. Pitz-Paal, Sand erosion on solar reflectors: Accelerated simulation and comparison with field data, *Solar Energy Materials and Solar Cells*, 145, Part 3, 303-313 (2016).
17. D. Schüler, S. Wilbert, N. Geuder, R. Affolter, F. Wolfertstetter, C. Prahl, M. Röger, M. Schroedter-Homscheidt, G. Abdellatif, A.A. Guizani, M. Balghouthi, A. Khalil, A. Mezrhab, A. Al-Salaymeh, N. Yassaa, F. Chellali, D. Draou, P. Blanc, J. Dubranna, O.M.K. Sabry, The enerMENA meteorological network – Solar radiation measurements in the MENA region, AIP Conference Proceedings, 1734 (2016) 150008.
18. http://www.dlr.de/sf/desktopdefault.aspx/tabid-7235/
19. N. Hanrieder, Determination of Atmospheric Extinction for Solar Tower Plants, Ph.D. thesis, RWTH Aachen 2016.
20. DIN 52348, Prüfung von Glas und Kunststoff, Verschleißprüfung - Sandrieselverfahren, DIN, 1985.
21. ISO 12103-1:2016, Road vehicles - Test contaminants for filter evaluation - Part 1: Arizona test dust, 2016.
22. F. Sutter, S. Ziegler, M. Schmücker, P. Heller, R. Pitz-Paal, Modelling of optical durability of enhanced aluminum solar reflectors, *Solar Energy Materials and Solar Cells*, 107, 37-45 (2012).
23. B. Weinzierl, A. Petzold, M. Esselborn, M. Wirth, K. Rasp, K. Kandler, L. Schütz, P. Koepke, M. Fiebig, Airborne measurements of dust layer properties, particle size distribution and mixing state of Saharan dust during SAMUM 2006, *Tellus B*, 61, 96-117 (2009).
24. T. Von Kármán, Mechanische änlichkeit und turbulenz, Nachrichten von der Gesellschaft der Wissenschaften zu Göttingen, Mathematisch-Physikalische Klasse, 1930, 58-76 (1930).
25. I. Hutchings, Transitions, threshold effects and erosion maps, *Key Engineering Materials, Trans Tech Publ*, 75-92 (1992).
26. P.H. Shipway, I.M. Hutchings, The role of particle properties in the erosion of brittle materials, *Wear*, 193, 105-113 (1996).
27. J.L. Routbort, A. Turner, The erosion rate of reaction-bonded SiC containing various amounts of free silicon, *Wear*, 84, 381-385 (1983).